



Multiscale simulation of field emission triode nanostructures

Ivan Sokolov, Ivan Vitchak, Nikita Kakorin, Nikolay Egorov, Konstantin Nikiforov*

Saint Petersburg State University, St. Petersburg, Russia, *k.nikiforov@spbu.ru

Presentation IVEW19
at virtual 7th ITG-IVEW
and 13th IVeSC, 2020
May 26-29, Bad Honnef

INTRODUCTION/MOTIVATION

Anode current of field electron emission (FE) triode is a function of two variables: voltage U_g between cathode and gate and voltage U_a between cathode and anode, i.e. $I_a = f(U_g, U_a)$. Important characteristics of triode operation in static mode [1] are the following differential parameters: slope of S_a value, which is equivalent to conductivity of an alternating current

$$S_a = \left. \frac{\partial I_a}{\partial U_g} \right|_{U_a = \text{const}}, \quad R_i = \left. \frac{\partial U_a}{\partial I_a} \right|_{U_g = \text{const}}$$

and the internal resistance R_i of the alternating current. The latter is an inverse of the slope characteristic in a diode, and for a triode it is defined as the ratio between anode voltage and anode current for constant gate voltage.

The gain of the triode to the anode current μ shows how many times stronger the gate potential affects the cathode current than the anode potential. The gain depends on the distribution of space charge:

$$\mu = SR_i = \frac{\partial I_a}{\partial U_g} \cdot \frac{\partial U_a}{\partial I_a} = - \left. \frac{\partial U_a}{\partial U_g} \right|_{I_a = \text{const.}}$$

The permeability of the gate D characterizes the penetration of the electric field through the gate of the anode to the cathode. Permeability is numerically equal to the ratio of charges induced on the cathode by the anode and by the gate, in the absence of current in the triode. It follows that the permeability depends on the geometry of the electrodes. The permeability of the gate D is expressed through the gain μ from the equation $\mu \approx 1/D$ (when $U_g < 0$).

Multiscale simulation of FE triode nanostructures under the study implies:

(A) Treatment as ideal FE device/system [2], when simulated emission characteristics are determined only by the geometry (smooth at microscale) of the system and the physics of emission from a surface that has fixed unchanging shape and a work function that does not vary significantly with local surface field or with emission current density.

(B) Treatment as non-ideal device/system due to current dependence in field enhancement factor (FEF) taking into account the complex geometry of surface at nanoscale, when increasing of field strength the effective FEF decreases [3].

LITERATURE DATA

Table I shows literature data on experimentally measured values of triode differential parameters or volt-ampere characteristics from which those values have been derived by formulas above. So this table presents a comparative study of various triode FE structures on the basis of an analysis of their differential parameters in the static mode of operation in an external electric circuit, both from experimentally measured current-voltage characteristics and from simulation results [4-19].

METHODS OF SIMULATION

Methods of mathematical and computer simulation in case (A) are based on a current function that is analogous to one used in hydrodynamics [20]. Finite-element method over a non-uniform mesh is used for electric field calculations and algorithms in Matlab PDE Toolbox and Comsol Multiphysics are implemented.

In case (B) mathematical model of nanostructured FE surface is implemented in the DAISI (Design of Accelerators, optImizations and Simulations [21]) with electrostatic and electromagnetic particle in cell methods, it allows to compute electric field on the rectangle mesh with good accuracy even for difficult geometry of computational domain. Deficiency of accuracy in extrapolation of difficult domain geometry by rectangle mesh is compensated by using cut cells method. The obtained result accuracy is not worse than the result accuracy using Comsol [22]. Modification has been performed, allowing simulations of devices in the FE mode with user defined initial energy distribution, because silicon carbide nanostructures under the study have bimodal energy spectra (see IVEW 24 presentation).

Table I. FE triode differential parameters in static mode for various structures.

Triode model description	Transconductance: $g_m = \frac{dI_a}{dU_g} U_a = \text{const}$	Triode internal resistance: $R_i = \frac{dU_a}{dI_a} U_g = \text{const}$	Triode gain: $\mu = \frac{dU_a}{dU_g} I_a = \text{const}$	Variation of current-voltage characteristics
Saturn model [4]	0.03–0.10 μS	56.18–500 MOm	1–6.25	U_a : 0–80 V U_g : 10–60 V
Nanotubes in Spindt's structure [5]. Emitter length: 15 μm . Mesh-anode distance: 20.5 μm . Mesh thickness: 3 μm . Cathode-anode distance: 2.5 μm . Cathode-anode distance: 400 μm [6].	0–73.99 μS	-	26–28	U_g : 20–55 V U_a : 20–200 V
Triode structures based on graphite mesh [7].	0–1.30 μS	20 MOm	-	U_g : 270–300 V U_a : 224–250 V
Spindt-like structure [8]. Emitter height 1 μm . Anode-cathode distance: 100 μm . CNT [9].	0.8 μS	-	-	U_g : -40–40 V U_a : 2.5 kV
The area of the triode is 2x2 μm . Emitter height 0.5 μm . Cathode-anode distance 100 μm . Anode-cathode distance: 25 μm . Grid radius 1.1 μm [10].	0–60 μS	4.33–60 MOm	-	U_g : 0–60 V U_a : 0–60 V
CNT [11]. Emitter radius: 250 μm . Emitter height 70–350 μm . Blade and tip triodes [12]. Distance between emitters: 10 μm . Emitter's radius of curvature: 0.5 μm . Emitter height: 10 μm . Cathode-anode distance: 50 μm .	0–1.15 μS	28–125 MOm	12.5–33.3	U_a : 0–350 V
CNT [11]. Emitter radius: 250 μm . Emitter height 70–350 μm . Blade and tip triodes [12]. Distance between emitters: 10 μm . Emitter's radius of curvature: 0.5 μm . Emitter height: 10 μm . Cathode-anode distance: 50 μm .	0–4.1 μS	-	-	U_g : 0.4–1.2 kV U_a : 2.5 kV
Tip emitter [13]. Anode-cathode distance: 600 μm	0–40 μS	-	-	U_g : 25–35 V U_a : up to 300 V
Tip emitter [14]. Anode-cathode distance: 600 μm	-	-	0–5.4	U_g : 1–10 V U_a : up to 50 V
Tip emitter [15]. Anode-cathode distance: 600 μm	0–4 μS	-	-	U_a : up to 400 V U_g : up to 50 V
CNT [16]. All measurements within 100 nm. Anode-grid distance: 100 nm.	0–1 nS	-	-	U_a : up to 50 V U_g : up to 35 V
Tip emitters [17]. Grid diameter: 3.5–4 μm . Emitter height: 4 μm .	0–290 μS	-	-	U_a : 500 V U_g : up to 140 V
Tip emitter [18]. Anode-grid distance: 0.2–0.3 cm. Grid diameter: 380 μm . Emitter above the grid by: 250 μm	0–0.0015 μS	40 MOm	-	U_a : up to 3 kV U_g : -40–140 V
Tip emitter [19]. Anode-grid distance: 0.2–0.3 cm. Grid diameter: 380 μm . Emitter above the grid by: 250 μm	0.01–0.1 μS	-	-	U_c : 1–8 kV U_g : 40–140 V
Tip emitter [19]. Grid radius is 2 μm . Emitter above the grid by: 0.5 μm . Emitter-anode distance: 0.05 cm.	0.01–0.1 μS	-	-	U_c : 1–8 kV U_g : 40–140 V

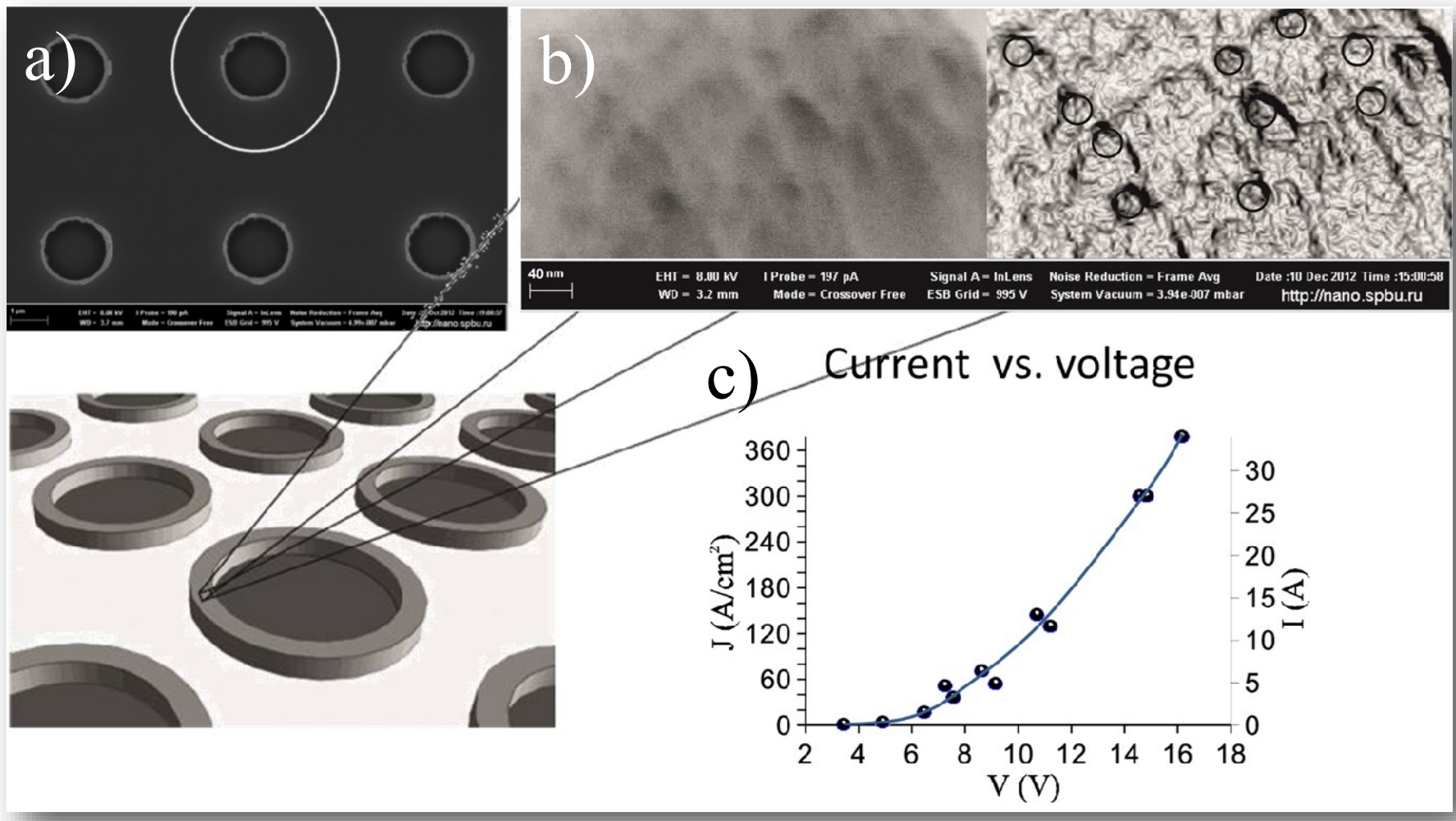


Fig. 1. Metal structures under the study: a) cell of a field emitters array with a cylindrical blade structure of vertical type [23]; b) image of edge-relief in SEM and after digital processing and pointing out geometrical non-homogeneities [3]; c) FE characteristics measured in diode configuration used for FEF estimation of emission surface in triode configuration.

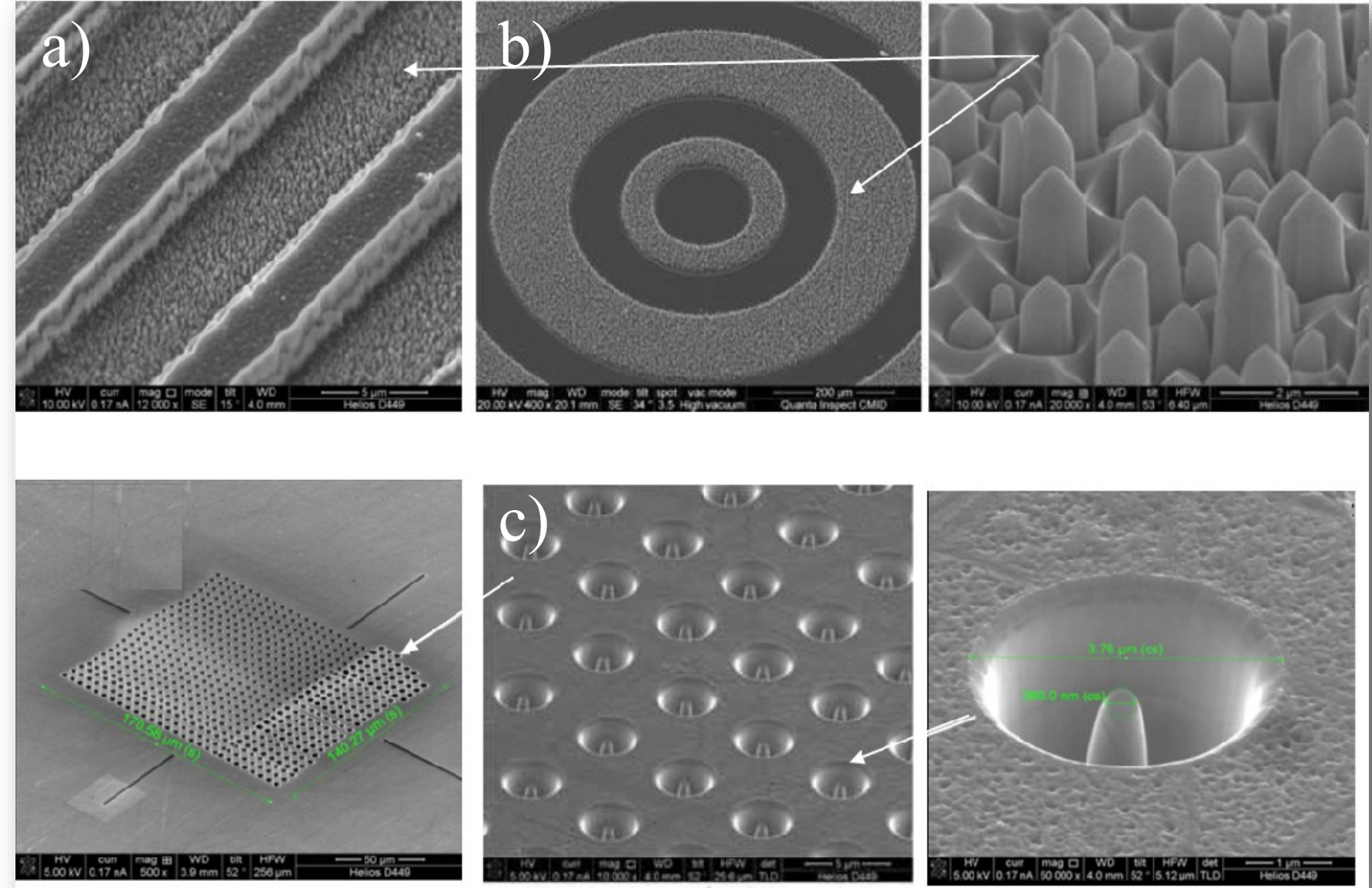


Fig. 2. Silicon carbide structures under the study: a) SEM image of linear blade triode structure [24]; b) SEM image of cylindrical blade structure [25]; c) FE array with cone-shape emitters [26].

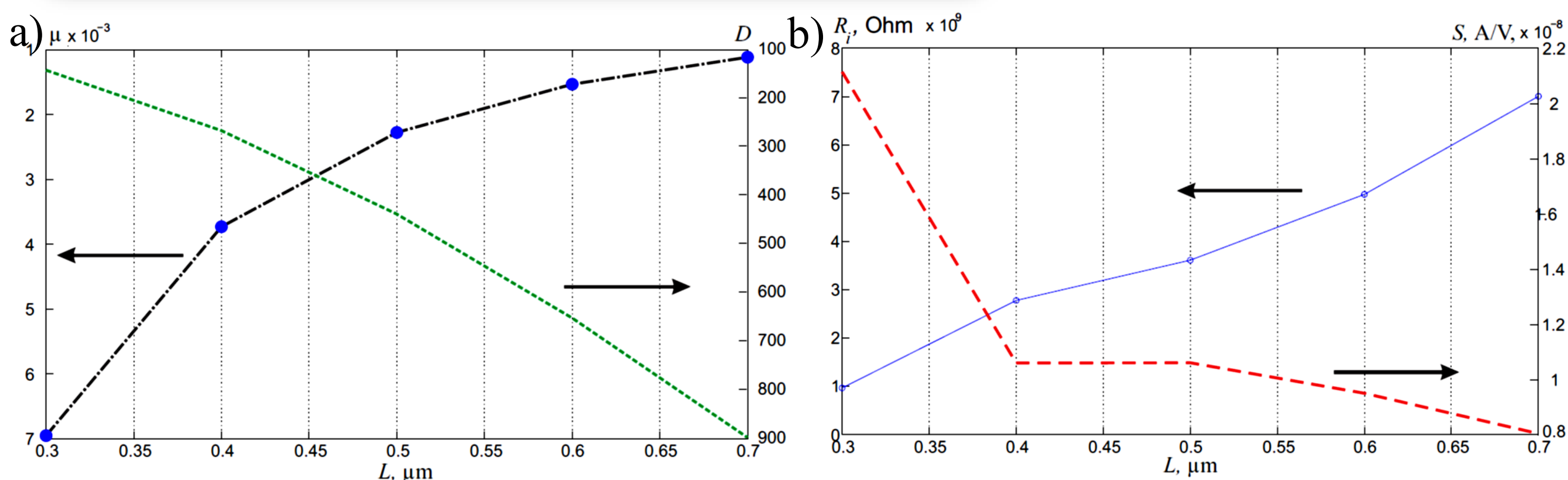


Fig. 3. Results of ideal device/system simulation in case (A) for cone-shape emitters triode: a) internal resistance and slope of anode volt-ampere characteristic vs anode-gate distance; b) triode gain and gate permeability vs anode-gate distance.

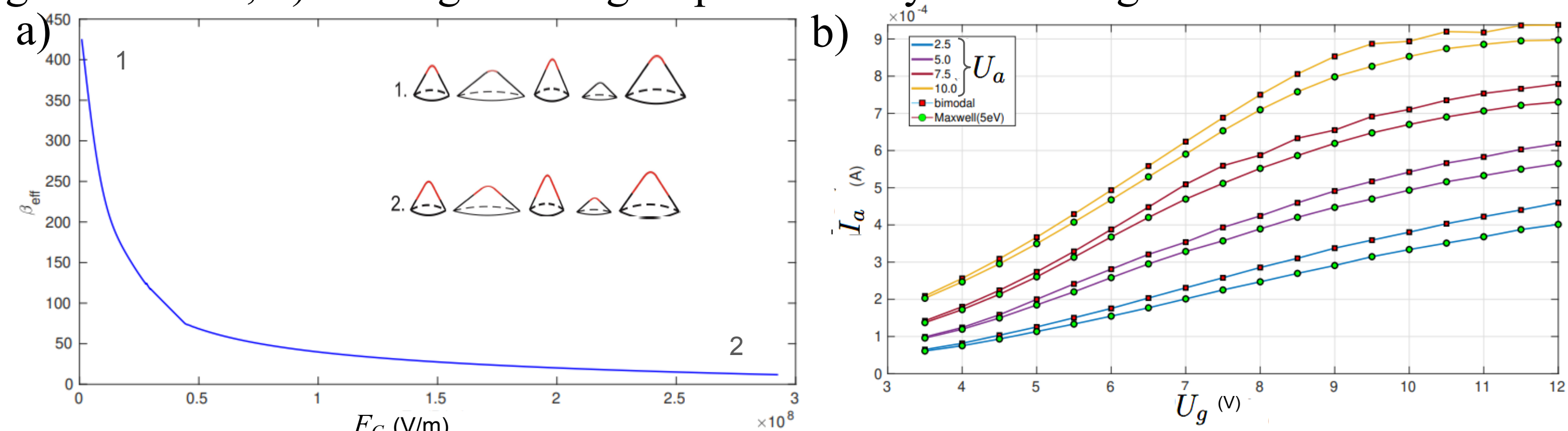


Fig. 4. Results of non-ideal device/system simulation in case (B) for cylindrical blade-shape emitters triode: a) current dependence in FEF, dependent on apex field; b) anode-gate characteristics at various anode voltages for two initial energy distributions: Maxwell's and bimodal spectra.

CONCLUSION

FE micro- and nanotriodes possess static differential parameters that are significantly (by orders of magnitude) different from the same characteristics of conventional electron lamps based on thermionic emission. Due to miniaturization and FE, using for generating of electron current in vacuum nanoelectronics triode structures, increasing the transconductance is an obvious necessity; additionally, transconductance plays an important role in high-frequency mode of triode devices operation.

REFERENCES

- [1] N. Egorov, E. Sheshin, Field emission electronics, Springer, 2017.
- [2] R. G. Forbes, Why converting field emission voltages to macroscopic fields before making a Fowler-Nordheim plot has often led to spurious characterization results // JVST B, 37(5), 051802, 2019.
- [3] A. N. Zartdinov, K. A. Nikiforov, Studying electric field enhancement factor of the nanostructured emission surface // Journal of Physics: Conference Series, 741, 012006, 2016.
- [4] C. W. Lu, C. L. Lee, A physical simulation model for field emission triode // IEEE Transactions on Electron Devices, 45(10), pp. 2238-2244, 1998.
- [5] T. Asano, Simulation of geometrical change effects on electrical characteristics of micrometer-size vacuum triode with field emitters // IEEE Transactions on Electron Devices, 38(10), pp. 2392-2394, 1991.
- [6] G. X. Li, B. Y. Zhong, J. Chen, Simulation of effects of geometrical parameters on the performance of a gated CuO nanowire cold cathode vacuum triode // 25th International Vacuum Nanoelectronics Conference (IVNC), p. 302, 2012.
- [7] D. Manoharan et al. The enhancement of the electron field emission behavior of diamond/CNTs materials via the plasma post-treatment process for the applications in triode-type vacuum field emission transistor // 29th International Vacuum Nanoelectronics Conference (IVNC), 2016.
- [8] Y. Gotoh, W. Ohue, Y. Yasutomo, H. Tsuji, Operational characteristics of vacuum triode with Hafnium Nitride field emitter arrays in harsh environments // 27th International Vacuum Nanoelectronics Conference (IVNC), 2014.
- [9] F. Brunetti et al. Field emission triode in a multifinger configuration with carbon nanotubes emitters // 2013 13th IEEE Conference on Nanotechnology (IEEE-Nano), pp. 397-400, 2013.
- [10] J. Koshorkhi, S. Mohajerzadeh, S. Darbari, Investigation of carbon nanotube-based field-emission triode devices on silicon substrates // IEEE Transactions on Nanotechnology, 11(6), pp. 1252-1258, 2012.
- [11] S. H. Hsu, W. P. Kang, S. Raina, J. L. Davidson, J. H. Huang, Nanodiamond Vacuum Field Emission Triode Signal Amplifier // 25th International Vacuum Nanoelectronics Conference (IVNC), p. 268, 2012.
- [12] P. Serbun, S. Rutkowski, A. Navitski, G. Muller, N. T. Hong, S. Lee, Field emission from carbon nanotube (CNT) arrays and triode test of single CNT columns // 2011 24th International Vacuum Nanoelectronics Conference (IVNC), p. 29, 2011.
- [13] A. I. Petrosyan, V. I. Rogovin, The numerical computation and studying of diodes and triodes with field emission // Actual Problems of Electron Devices Engineering (APEDE), 2010 International Conference on Saratov, Russia, 2010.
- [14] S. H. Hsu, W. P. Kang, J. L. Davidson, J. H. Huang, and D. V. Kerns, Performance characteristics of nanocrystalline diamond vacuum field emission transistor array // Journal of Applied Physics, 111(11), 114502, 2012.
- [15] S. H. Hsu, W. P. Kang, S. Raina, J. H. Huang, Nanodiamond vacuum field emission device with gate modulated triode characteristics // Applied Physics Letters, 102(20), 203105, 2013.
- [16] S. H. Hsu, W. P. Kang, J. L. Davidson, J. H. Huang, D. V. Kerns, Nanodiamond Vacuum Field Emission Integrated Differential Amplifier // IEEE Transactions on Electron Devices, 60(1), pp. 487-493, 2013.
- [17] D. Nicolaescu, V. Filip, S. Kanemaru, J. Itoh, Modeling of field emission nanotriodes with carbon nanotube emitters // Proceedings of the 14th International Vacuum Microelectronics Conference, pp. 39-40, 2001.
- [18] D. Palmer et al. Silicon field emitter arrays with low capacitance and improved transconductance for microwave-amplifier application // Journal of Vacuum Science & Technology B, 13(2) pp. 576-579, 1995.
- [19] H. H. Busta, D. W. Jenkins, B. J. Zimmerman, J. E. Pogemiller, Collector-induced field emission triode, IEEE Transactions on Electron Devices, 39(11), pp. 2616-2620, 1992.
- [20] H. H. Busta, J. E. Pogemiller, B. J. Zimmerman, Collector-assisted operation of micromachined field-emitter triodes // IEEE Transactions on Electron Devices, 40(8), pp. 1537-1542, 1993.
- [21] K.A. Nikiforov, N.V. Egorov, M.F. Saifullin Mathematical simulation of a diode system with a field-emission matrix cathode // Technical Physics 60(11), 2015, 1626.
- [22] K.A. Nikiforov, Mathematical model and software complex for computer simulation of field emission electron sources // AIP Conference Proceedings, 1648, 450014, 2015.
- [23] V. Altsibeyev, Configurable code for beam dynamics simulations in electrostatic approximation // 2016 Young Researchers in Vacuum Micro/Nano Electronics (VMNE-YR), St. Petersburg, 2016.
- [24] V. Ponomarev, V. Altsibeyev, Development of 2D Poisson equation C++ finite-difference solver for particle-in-cell method // Stability and Control Processes in Memory of V. I. Zubov (SCP), St. Petersburg, pp. 195-197, 2015.
- [25] K. A. Nikiforov, N. V. Egorov, M. F. Saifullin, Mathematical simulation of a diode system with a field-emission matrix cathode // Technical Physics, 60, no. 11, pp. 1626-1631, 2015.
- [26] A. V. Afanasiev, V. A. Golubkov, A. S. Ivanov, V. A. Ilyin, V. V. Luchinin, V. A. Kurtash, V. Serkov, Investigation of a Possibility of Development of a Triode Type Electron Field Source Based on 4H-SiC-Structure with a Semi-Insulating Epitaxial Layer // Nano and Microsystems Technology, 20, pp. 719-726, 2018 (doi: 10.17587/nmst.20.719-726 in Russian: Nano-1 Mikrosistennaya Tekhnika).
- [27] A. V. Afanasiev, V. A. Golubkov, A. S. Ivanov, B. V. Ivanov, V. A. Ilyin, A. V. Korlyakov, A. V. Lagosh, Family of Silicon Carbide Solid State, Vacuum and Microelectronic Switches for Harsh Environments // Microwave Electronics and Microelectronics, 1(1) pp. 80-84, 2017 (in Russian, Proceedings of VI Pan-Russian conference, St. Petersburg, SPETU "LETT", May 29-June 1 2017).
- [28] M. A. Kuznetsova, V. V. Luchinin, Focused Ion Beam Machining of SiC Field Emitters // Nano and Microsystems Technology, 12(149), pp. 35-40, 2012 (in Russian, Nano-1 Mikrosistennaya Tekhnika).
- [29] K. A. Nikiforov, Z. R. Gallyamov, Modelling of static mode characteristics of a thin-film vacuum nanotriode // Journal of Physics: Conference Series, 643(1), 012123, 2015.

Acknowledgments: The reported study was funded by RFBR, project number 20-07-01086.